

Ergodic Divertor Experiments On The Route To Steady State Operation Of Tore Supra

Tore Supra team presented by Ph. Ghendrih

Association Euratom-CEA sur la fusion, CEA Cadarache, 13108 St Paul Lez Durance, France

e-mail contact of main author : Ghendrih@drfc.cad.cea.fr

Abstract. Ergodic Divertor operation on Tore Supra is characterised by good performance in terms of divertor physics. Control of particle recirculation and impurity screening are related to the symmetry both poloidally and toroidally of the shell of open field lines and to its radial extent, $r \sim 0.16$ m. Feedback control of the divertor plasma temperature has led to controlled radiative divertor experiments. In particular, good performance is obtained when the plasma is controlled to be a temperature comparable to the energy involved in the atomic processes, (15 to 20 eV). For standard discharges with 5 MW total power and ICRH heating, the low parallel energy flux ~ 10 MW m⁻² is reduced to ~ 3 MW m⁻² with nitrogen injection. This is achieved at a modest cost in core dilution, $Z_{\text{eff}} \sim 0.3$. Despite the large volume of open field lines (~ 36 %) the Ergodic Divertor does not reduce the possible current in the discharge since stable discharges are achieved with $q_{\text{sep}} \sim 2$. It is shown that the reorganisation of the current profile in conjunction with a transport barrier in the electron temperature on the separatrix stabilises the (2,1) tearing mode. Confinement follows the standard L-mode confinement. In a few cases at high density and with no gas injection (wall fuelled discharges), "RI-like" modes are reported with modest increase in confinement (~ 40 %). Despite the lack of core fuelling on Tore Supra, high densities during ICRH pulses can be achieved with Greenwald fractions $f_G \sim 1$. Compatibility with both ICRH and LH is demonstrated. In particular long pulse operation with flat top in excess of 20 s are achieved with LHCD.

1. Introduction

Steady state operation requires a high level of integration of both physics and technology. Experiments on Tore Supra indicate that power exhaust is among the very first issue to be solved in order to tackle other aspects of long pulse operation such as current drive and even improved confinement [1,2]. Many configurations, mostly limiter configurations, have been investigated on Tore Supra during the first ten years of operation [1]. The circular cross section of Tore Supra ($R \sim 2.39$ m, $a \sim 0.79$ m) does not allow for significant shaping of the plasma without a very strong loss of confinement volume. In order to give access to divertor physics, the machine has been equipped with the so-called Ergodic Divertor.

While the axisymmetric divertor is based on the generation of a large poloidal component of the magnetic field, the ergodic divertor is used to generate a radial perturbation. The latter is helicoidal and is therefore resonant on magnetic surfaces with rational safety factors [3]. The number of identical coils implemented in the machine determines the main toroidal mode number, $n = 6$. A proper design of the coil then defines the poloidal spectrum. The octopolar coils of Tore Supra generate an $m = 18 \pm 6$ spectrum that defines the operating point of the edge safety factor : $q_{\text{edge}} \sim 3$. The high poloidal wave number governs a sharp decrease of the magnetic perturbation towards the plasma core. As a consequence, the non-linear interaction of the resonant modes generates a stochastic boundary which extends typically between the $q = 2$ surface at $r \sim 0.8$ and the $q \sim 3$ surface at the very edge.

First operation of the ergodic divertor was performed in 1988 with a very reduced set of dedicated diagnostics, actively cooled target plates and very little protection of the coil casing. The 1996 upgrade significantly improved the diagnostic capability and reinforced the heat extraction capability [4]. In particular the front face was fully covered with 20 mm thick CFC tiles inertially cooled between shots. The 42 new target plates have a vented structure with

B₄C coating of the actively cooled CuCrZr tubes. These were designed to sustain up to 9 MW m⁻² in steady state [4].

After the final year of operation of the Tore Supra ergodic divertor, a general survey of the experimental investigation can be presented. Section 1 is dedicated to the divertor performance, including some geometrical features of the stochastic boundary, Section 1.1, efficiency of this shielding layer in terms of control of particle recirculation, Section 1.2, and, control of the parallel heat flux to the target plates, Section 1.3. Section 2 is dedicated to the integration of core physics with a stochastic boundary, including the operational window in terms of plasma current, energy confinement and access to high Greenwald ratios, Section 2.1, and, finally long pulse operation with LHCD, Section 2.2.

2. Divertor physics with the Ergodic Divertor

2.1 Connection length distribution in the stochastic boundary

A statistical analysis of infinite and homogeneous stochastic systems provides several characteristic properties of the stochastic boundaries that are readily computed knowing the spectrum of the magnetic perturbation [4]. An alternative description of the stochastic boundary can be achieved by computing the connection length of a series of points in the stochastic boundary. These are computed with the Mastoc code [5]. To separate the co and counter connection lengths, they are given opposite signs, LHS figure of FIG. 1.

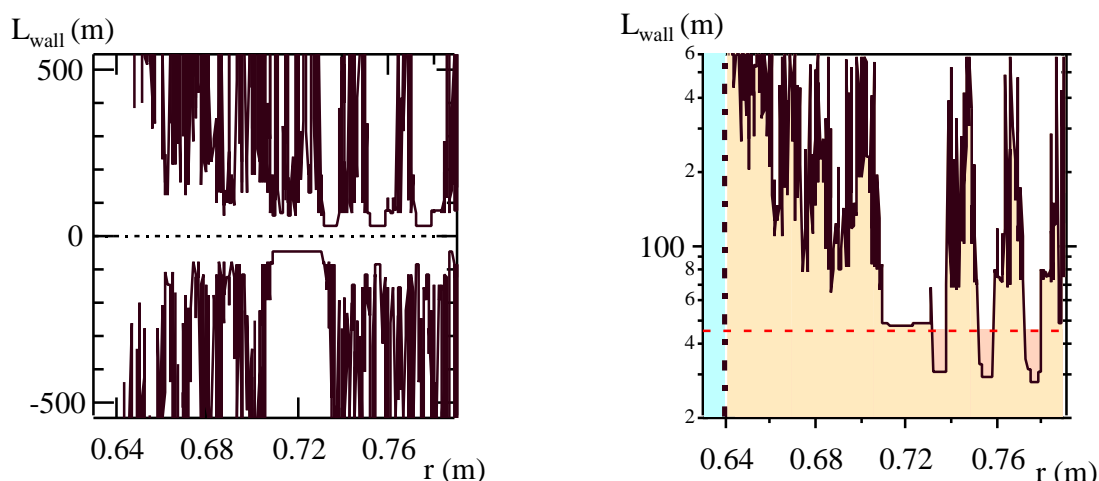


FIG. 1 : Computation of the connection length to the wall L_{wall} for a radial scan from the bottom of the machine, $\theta = -\pi/2$ and at $\varphi = 20^\circ$ from a divertor coil. Left figure L_{wall} in the co (positive value) and counter (negative value) for the same initial conditions. Right minimum of the co and counter connection lengths (black curve) compared to a typical connection length of $2\pi qR$ (dashed red line). The colour code defines the various transport regimes, closed magnetic surfaces (light blue), the “ergodic” region (yellow) and the “laminar” region (pink).

In this calculation the upper limit of the field line excursion is set to $\pm 100 / 6$ toroidal rotations, equivalent to ~ 600 m. A striking feature of this result is the complexity of the connection length behaviour. The latter is typical of stochastic systems. A second outstanding feature is the very long connection lengths which are found up to 0.16 m from the wall ($a_{ED} = 0.79$ m). One can also observe the strong divergence of L_{wall} towards the separatrix at

$r_{\text{sep}} \sim 0.64$ m. Finally, one finds that the minima in the connection length are well organised which indicates that the stochastic feature do not prevail along these short distances. Although the local L_{wall} values will be very sensitive to the location of the initial point or to slight changes in the magnetic equilibrium, the qualitative features are very robust. This is summarised on the RHS figure of FIG. 1, where the minimum connection length between the co and counter values is plotted versus the minor radius. In this plot the colour code indicates the various transport region that constitute the stochastic boundary. The blue area is characterised by closed magnetic surfaces ($L_{\text{wall}} \rightarrow \infty$) and dominated by cross-field transport [6]. The last closed magnetic surface defines the separatrix and for standard operation, $B_T \sim 3$ T and full divertor current $I_{\text{ED}} \sim 45$ kA, is located at $r_{\text{sep}} = r_{\text{sep}} / a_{\text{ED}} \sim 0.8$. Note that the plasma radius is defined as a_{ED} , namely the radius of the CFC tiles on the divertor coil. The regions with short connection lengths, typically shorter than a standard connection length $2 \cdot qR$ (~ 45 m on Tore Supra) are governed by parallel transport very much in the fashion of the axisymmetric divertor [7]. This characterises the so-called “laminar” transport region [4] with pink colouring on FIG. 1. Typically, in such a radial scan, one finds 3 main regions of such laminar transport with radial extents in the 0.01 m range, i.e. comparable to standard SOL width in L-mode operation. The region with a yellow colouring is called the “ergodic” region, transport in this region is a balance between parallel and transverse transport [4]. A consequence of this typical structure is that the core plasma is shielded by a large SOL, 0.15 m large, that is symmetric both poloidally and toroidally. A significant fraction of the radial extent, ~ 20 %, is characterised by very short lifetime due to a very short connection length to the wall.

2.2 Control of particle recirculation

The aim of divertor configurations is to control particle recirculation by generating a radial gap between the last closed magnetic surface and the recycling areas. Three outstanding results have been observed in the axisymmetric divertor. First, impurities generated at the divertor target plates are effectively controlled in L-mode operation [8]. Second, mechanical closure of the divertor volume enhances the control of the neutral deuterium leading, in particular, to a strong increase of neutral pressure in the divertor [9]. Third, the thin SOL away from the divertor volume appears to be inefficient in shielding the core plasma from particle release by the wall [10].

The Tore Supra divertor is an open divertor where particle control can only be achieved by the plasma itself. The core plasma shielding has been characterised by the divertor tightness, namely the capability to reduce the neutral particle flow to the core plasma. This is defined as the ratio of the divertor density to the core volume averaged density [11]. It has long been found and reported in the literature [12,3] that the ergodic divertor is effective in lowering the impurity inflow, both for metallic impurities [112] and light impurities such as carbon [3]. Control of main ion species, D or He, provides another measure of the divertor performance. It is found in particular that the turning points in terms of core density between the various density regimes, from linear to high-recycling and from high-recycling to detached [13] are characteristic of the divertor tightness [14]. Main results of the Ergodic Divertor experiments are low values of the core density at the transition from high recycling to detached plasma despite low values of the tightness, typically of the order of 0.3 in ohmic shots [11]. The latter feature is in fact governed by the very low parallel heat flux achieved in the stochastic boundaries as also evidenced on LHD [15]. In these cases with weak plasma pressure, it is also found that the rollover to detachment occurs at rather high plasma temperature typically

$T_{\text{div}} \sim 10$ eV [11,14]. Detachment is defined here as the departure from the high recycling regime, i.e. from the quadratic scaling of the ion flux versus the core density [9].

Further evidence of the control of particle recirculation is given by the analysis of the particle flux to the target plate, measured with a Langmuir probe and the measure of the neutral inflow computed from a full image of the target plate in H light. For both signals one finds the same dependence in a density scan, and, for reasonable estimates of the wetted surface, quantitative agreement is observed [12]. Direct analysis of the H image also exhibits a localised neutral inflow, FIG. 2. The H light plotted along a chord transverse to the target plate and along a chord parallel to the target plate is well localised on the target plate. In the transverse direction about 60 % of the target plate is actually wetted, hence the reduced size of the H maximum compared to the 0.1 m width of the target plate. The local minimum in the vicinity of $d = 0$ corresponds to a gap of the vented structure. Clearly the gap is comparable to atomic scales so that the minimum is not very pronounced. In the parallel direction, the chosen chord runs through an area which is orthogonal to the field lines (at $d_{\parallel} \sim 0$). This governs a focussing of the particle and energy flux.

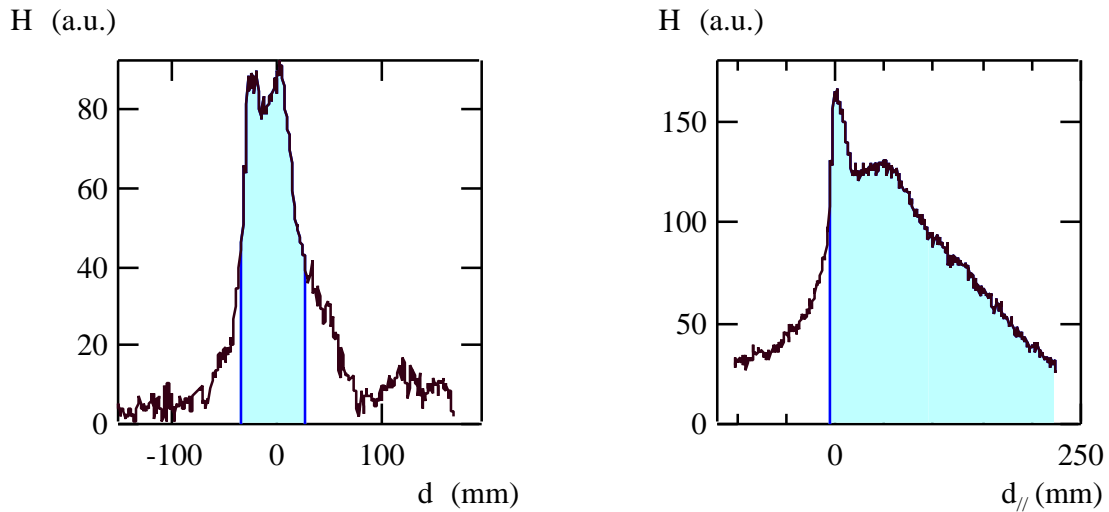


FIG. 2 : Profiles of H_{α} light transverse (LHS) and parallel (RHS) to the target plate. The coloured regions correspond to the visible extent of the target plate, typically 60 mm poloidally and 220 mm in the parallel direction.

The sharp peak in H light is indicative of this effect. Towards the negative values, one observes an exponential decay. This region has little particle source since the plasma facing components are withdrawn radially compared to the target plate. Towards the positive values a more complex decay is observed due to the particle recycling on the target plate. The latter decays away as d_{\parallel} increases since the target plate is radially inclined outwards governing a reduction of the ion flux.

The clear peaking of the ionisation source in the vicinity of the target plate demonstrates that particle channelling by the Ergodic Divertor is effective and that recirculation of particles is controlled despite the open geometry. The divertor is tight and plasma shield effective.

2.3 Low Energy flux to the target plate

The Ergodic Divertor is equipped with high heat flux components that are actively cooled. Performance of such a heat sink is associated with low time constants to reach equilibrium, typically in the range of a couple of seconds for the CuCrZr structure. The B₄C coating has a much faster time response of the order of 40 ms, i.e. a time frame of the Infra-Red imaging system. Furthermore, the design value of the maximum heat load in steady state is of $Q_{\text{Exhaust}} \sim 9 \text{ MW m}^{-2}$, very similar to design values of Next Step devices. As a consequence control of the energy flux to the divertor is compulsory. The Ergodic Divertor does not allow for flux expansion as the axisymmetric divertor does. As a consequence, the angle between the plasma facing components and the magnetic field cannot be varied. This angle is typically of 8° for the vented target plates as implemented. The upper bound of the parallel heat flux to the target plate is then $Q_{\parallel} \sim 65 \text{ MW m}^{-2}$. Radiation is a standard means to reduce the parallel heat flux in order to meet the technological constraints. It is therefore appropriate to analyse the divertor performance in terms of its capability to lower the energy flux to the target plate at minimum impact on core performance, typically Z_{eff} for radiative plasmas.

A striking feature when considering the parallel energy flux Q_{\parallel} to the Ergodic Divertor is the low values routinely observed. The highest energy fluxes have been recorded for low density shots with Lower Hybrid Current Drive (LHCD). They remain with $Q_{\parallel} < 20 \text{ MW m}^{-2}$. A possible interpretation would be a significant enhancement of cross-field transport leading to a large increase of the wetted surface and no peaking of the power deposition. Evidence from particle recirculation FIG. 2 indicates that recycling fluxes are localised on the target plates. Since energy deposition is convective by nature, localised particle fluxes are a signature of localised energy fluxes. Another experimental evidence of localised deposition is given by off-normal operation of Lower Hybrid. Indeed, when the density in the vicinity of the LH grill is too large, a small fraction of the LH energy is coupled to boundary electrons and generates an electron beam with electrons of $\sim 200 \text{ eV}$ [14,16,17]. This beam remains focussed over several meters of parallel transport so that parallel energy fluxes $> 150 \text{ MW m}^{-2}$ have been recorded at the strike point defined by parallel connection between the LH grill and the target plate [17]. The duration of this off-normal heat pulse was short enough to limit the damage to melting of typically 10 mm * 10 mm of the B₄C coating which led to a disruptive termination of the discharge. The lowering of the parallel energy flux thus appears to be linked to transport properties of the ergodic region and not to an enhancement of cross-field transport in the vicinity of the plasma facing components.

Numerous experiments have been carried out to control Q_{\parallel} . A specific scenario has been routinely used during the last experimental campaign to evaluate radiative performance at given divertor temperature. To this end the divertor temperature measured by two Langmuir probes was used to monitor the gas injection [18,19], FIG. 3. On this characteristic time trace, the divertor temperature is lowered with a controlled ramp-down and set to a value in the range 15 to 20 eV. The increase of the gas injection Γ_{inj} is clearly correlated to the rise in divertor temperature. Some oscillations of divertor temperature remain due to the slow response of the gas injection system. A consequence of this scenario is that the core density is determined by the temperature of the divertor plasma. Clearly noticeable on FIG. 3 is the rollover of the particle flux to the divertor Γ_{div} while volume averaged density $\langle n_e \rangle$ still increases. This detachment also leads to a sharp drop of Γ_{inj} that one readily interprets as a lowering of the screening capability of the Ergodic Divertor. It is interesting to note that the gas injection required for this feedback control is typically 4 % of the total recycling particle flux.

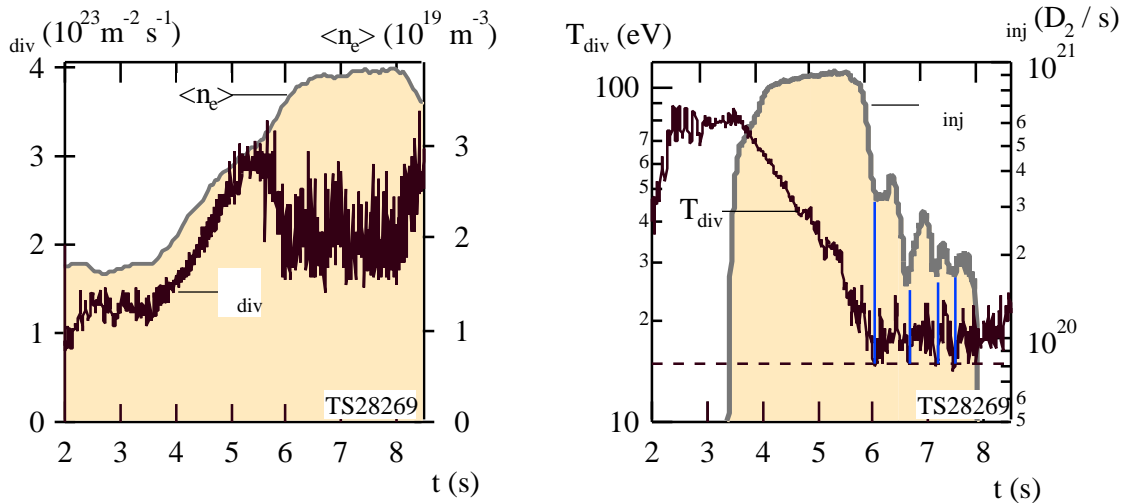


FIG. 3 : Gas injection control of the divertor temperature. On the left figure impact of this feedback scheme on the particle flux at the divertor target plate and on the volume averaged core density. On the right hand figure, response of the divertor plasma temperature to the gas injection Φ_{inj} .

On FIG. 4 are plotted the results from a series of shots with a total injected power of 5 MW and injection of extrinsic impurities to further reduce Q_{\parallel} . On the RHS figure is reported the dependence of Q_{\parallel} as a function of the power to the divertor $P_{\text{Total}} - P_{\text{Rad}}$. P_{Rad} is measured by a set of bolometer cameras located toroidally 20° away from a divertor coil. Extrapolation indicates that for a radiated fraction of 0 % the energy flux is limited to less than 20 MWm^{-2} . At 60 % of radiated power, Q_{\parallel} is reduced to 5 MWm^{-2} , a level that can be dealt with even in the case of field lines orthogonal to the target plates.

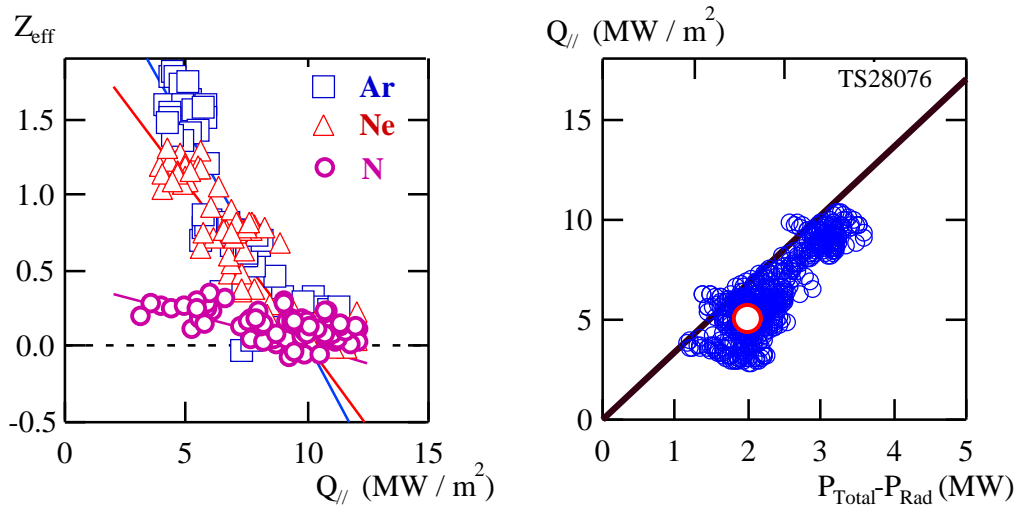


FIG. 4 : Cost in Z_{eff} . Z_{eff} to lower the parallel energy flux(LHS), and, for a given shot with nitrogen injection, correlation of the decrease of Q_{\parallel} with the power to the divertor, $P_{\text{Total}} - P_{\text{Rad}}$, (RHS).

Data on the RHS figure corresponds to a shot with nitrogen injection. Cost in Z_{eff} of this injection is reported on the left figure of FIG. 4 and compared to injection of neon and argon. In all cases a comparable achievement in terms of lowering of Q_{\parallel} is observed. However, the

cost in Z_{eff} is significantly different. The linear dependence between Z_{eff} and Q_{\parallel} allows one to illustrate this point by determining the cost in core dilution of a 10 MW m^{-2} decrease of Q_{\parallel} . Neglecting other sources of core dilution (He ash and intrinsic impurity contamination), one finds a lowering of the fusion energy of 40 % in the case of argon, 30 % in the case of neon and 15 % in the case of nitrogen. (These correspond to contributions to the core electron density of 23 % for Ar, 16 % for Ne and 7 % for N). It is thus clear that the choice of an impurity that radiates in the divertor volume, and the feedback of the divertor plasma temperature to the appropriate temperature range, leads to the lowest contamination of the core plasma [18,20]. A simple extrapolation from the working point at 5 MW m^{-2} to 50 MW m^{-2} hence to fluxes to the component lower than 7 MW m^{-2} shows that 50 MW of total injected power could be accommodated ($P / R \sim 20 \text{ MW / m}$). At given divertor plasma temperature this input power would yield a factor 3 in core density. Following the Multi Machine Scaling [21] a reduction of $(Z_{\text{eff}}-1)$ of a factor close to 10 would then be required to remain at 60 % of radiated power. As a consequence of the favourable trend in heat extraction, the actively cooled components have been very reliable without a single loss of coolant during the 10 years of operation.

3. Integration of core physics and stochastic boundaries

3.1 Standard performance in confinement and stable MHD operation

The Ergodic Divertor was designed for high plasma current operation, a choice that still provides the highest core energy confinement. As a consequence the poloidal spectrum of the Ergodic Divertor is optimised for a safety factor $q_{\text{edge}} \sim 3$ ($q_{\text{edge}} = q(a_{\text{ED}})$) at low β , and allows for an upward shift as β is increased due to a Shafranov shift effect when the coils are located on the low field side [22]. While this resonance effect has been documented experimentally [3], only recent investigation was dedicated to determining the location of the separatrix.

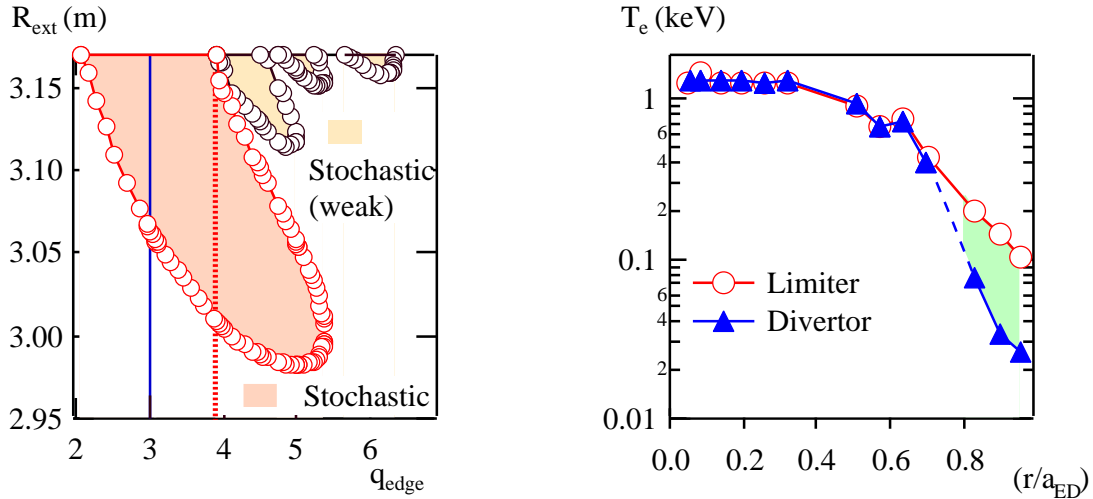


FIG. 5 : Radial extent of the stochastic boundary in the midplane, $R_{\text{ext}} = R + r$, starting from the major radius of the ED coil $R_{\text{ext}} = 3.17 \text{ m}$ as a function of the edge safety factor (LHS). On the RHS figure, electron temperature versus minor radius for limiter and Ergodic Divertor shots. The region coloured in green is that of the divertor volume with low electron temperature.

One means has been to determine the value of q_{edge} at the transition from the limiter to the divertor configuration during current ramp-up. The result of the theoretical analysis is shown

on FIG. 5. Coloured areas on the LHS figure indicate the radial extent of the stochastic regions. Peak of the stochasticity is located on the $q = 3$ surface. During current ramp-up, this surface moves towards the wall. This leads to the shape of the pink area. The outer separatrix which bounds this stochastic region reaches the wall at $q_{\text{edge}} \sim 4$. This corresponds to the experimental value for the transition from limiter to divertor configuration [22]. The operational domain of the Ergodic Divertor thus extends from $q_{\text{edge}} \sim 4$ to $q_{\text{edge}} \sim 2$ when the main separatrix, i.e. between the core plasma and the divertor plasma, moves out of the plasma. Evaluation of this separatrix position also indicates that it remains in the vicinity of the $q = 2$ surface in all this standard range of operation. Interestingly enough, this standard operation exhibits stabilisation of the (2,1) tearing mode. However, it is shown that further increase of the penetration of the separatrix eventually triggers a disruption due to the (3,2) tearing mode [20]. Analysis of the stability of these modes indicates that the effect is not governed by direct interaction of the Ergodic Divertor modes with the MHD modes but rather to an indirect control via the current profile. In particular, stability of the (2,1) tearing mode is associated to the electron temperature barrier that build-up at the separatrix [3], FIG. 4.

The existence of such a barrier on the electron temperature, also explains the properties in terms of energy confinement. In particular, one finds that for a given density, the core temperature is unaffected. The energy content of the discharge is thus very similar to that of limiter shots and thus follows the standard L-mode scaling on Tore Supra [23]. The large volume of open field lines, typically 36 %, does not lower the energy content of the discharge. Measurements of the density fluctuations have shown that the core fluctuations (≈ 0.8) are the same in limiter and Ergodic Divertor shots [24]. A decrease is observed on the divertor volume (0.8 \rightarrow 1). The k-spectrum indicates that only the large modes are stabilised, the modes at larger k showing a small increase [24]. These features are recovered by 3D simulation of ballooning turbulence with the Ergodic Divertor [25]. Although density fluctuations decrease in these simulations, it is shown that transport exhibits a slight increase due to the increase of the electric field fluctuations [25]. This result agrees with the analysis of the attached plasmas which indicate that cross-field transport is not modified by the stochastic boundary. However, at high density, in the rollover to detachment, probe measurements of ion saturation fluctuations exhibit a large increase [26]. Some change in cross-field transport in the stochastic boundary could be associated to the detachment process.

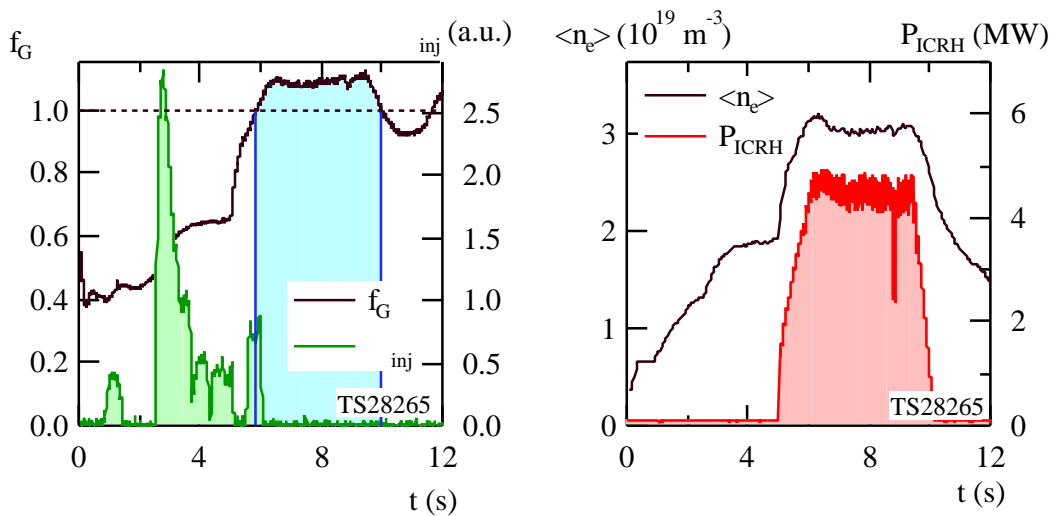


FIG. 6 : High density operation with ICRH heating, Greenwald fraction and gas injection (RHS), volume averaged density and ICRH power (LHS).

In several shots performed with no gas injection (natural density due to large wall fuelling), some confinement improvement is observed during the ICRH pulse. These shots are similar to the so-called "RI-like" shots achieved in limiter discharges [27]. During low field operation, $B_T \sim 1.5$ T, shots of this family, with modest improvement with respect to L-mode scaling [23] ($H_{L96} \sim 1.2$), are characterised by strong increase of the core density during the ICRH pulse (2nd harmonic heating in the H-minority scheme [28]). Greenwald fractions of the order of 1 are obtained, FIG . 6. For this shot low field shot, a value of n_N of 1.2 was reached.

3.2 Long pulse with Lower Hybrid Current Drive

Compatibility between magnetic perturbations and Lower Hybrid Current Drive could be questionable. In practise coupling of LH power did not rise difficulties and current drive efficiency comparable to limiter shots achieved [3] (on LHCD physics see [29]). Investigation of long pulse operation with the Tore supra Ergodic Divertor was subject to 2 limitations.

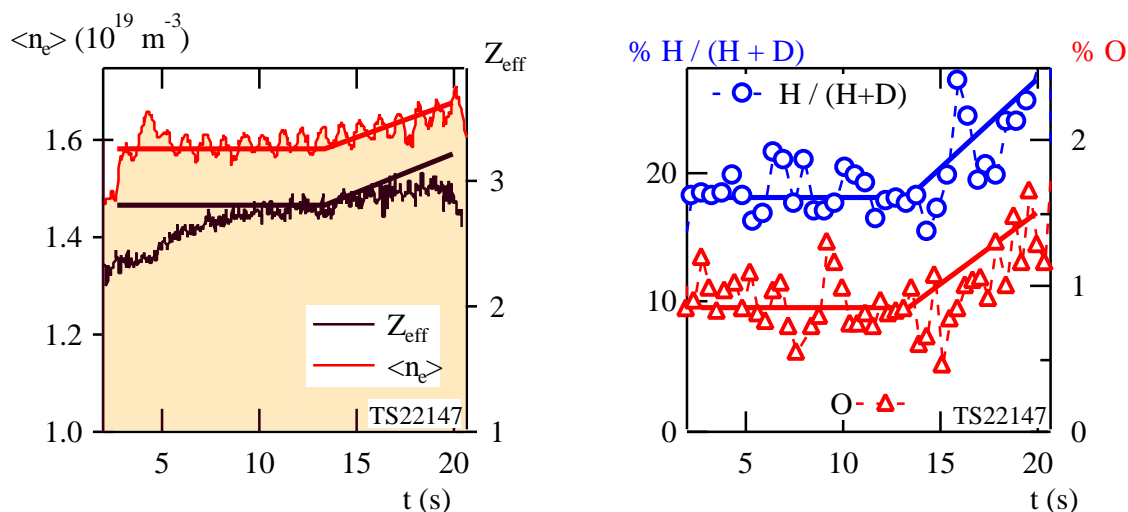


FIG. 7 : Time traces during flat top of LHCD current driven shot, volume averaged density and Z_{eff} (LHS), hydrogen fraction and oxygen concentration (RHS).

Owing to the cooling of the divertor coil, the pulse length was restricted to less than 30 s. Furthermore, operation at $q_{\text{edge}} \sim 3$ required large current generation and therefore large LH power. The limited power available was very marginal to achieve 30 s and certainly did not allow zero loop voltage operation. Longest flat top achieved was of 20 s. However, a disruption occurred during ramp down at ~ 25 s (for a programmed waveform of 28 s). We shall concentrate here on a similar shot with 17 s flat top, and soft landing at ~ 25 s. Parameters of the shot are $B_T \sim 3\text{T}$, $I_p \sim 1.4$ MA, $P_{\text{LH}} \sim 3.7$ MW, and $\langle n_e \rangle \sim 1.6 \cdot 10^{19} \text{ m}^{-3}$. A 1 Hz, 20 kA modulation of the plasma current was used. As during limiter long pulses, the density exhibits a slow increase after roughly 13 s of steady behaviour [30], FIG. 7.

Modulations of the density have the same frequency as the plasma current but with a $\pi/2$ shift. Since the largest shift is observed on interferometer chords closest to the centre, one can interpret this shift as a particle lifetime of 250 ms, much shorter than the evolution time of the density. A similar trend is seen on Z_{eff} , the final rollover being governed by a decrease of the carbon concentration (~ 5 %) as the density rises. As in long limiter pulses, one also observes a rise of the hydrogen fraction $n_{\text{H}} / (n_{\text{H}} + n_{\text{D}})$ from less than 18 % to about 30 %, FIG. 7. Rise of the oxygen concentration also starts at 13 s. This data can be understood as water desorption from components some distance from the plasma and which experience a temperature rise due to insufficient cooling.

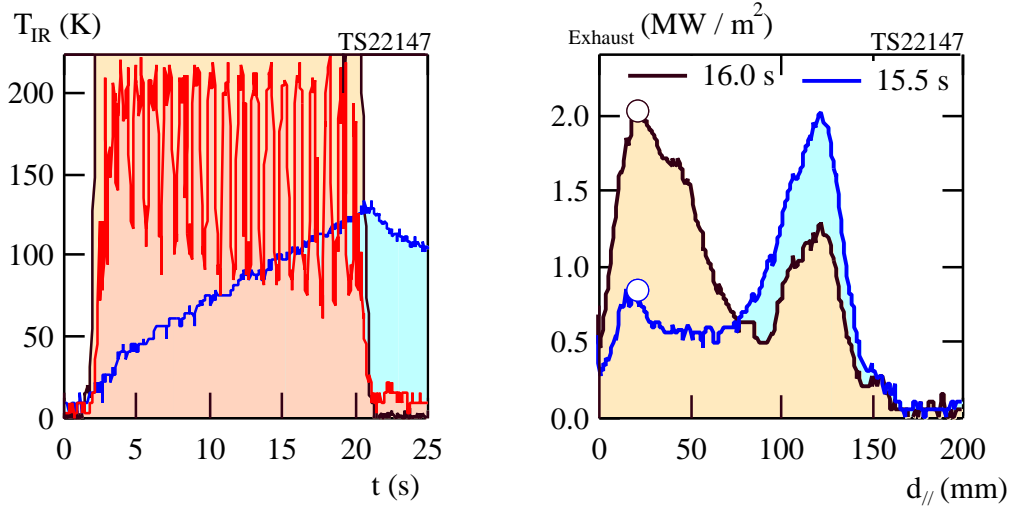


FIG. 8 : Time traces of the temperature variation of a point on the target plate (red curve) and of a point on an uncooled CFC protection tile (blue curve), the black line and yellow colouring corresponds to the LH pulse (LHS). RHS figure, profile of the exhaust energy flux $Exhaust$ along a target plate in the // direction. The circles indicate the location of the point of the target plate used in the time trace of the LHS figure. The profiles are modulated at the same frequency as I_p .

When analysing the behaviour of the Ergodic Divertor plasma facing components, FIG. 8, one finds that the actively cooled target plates exhibit a modulation of the surface temperature with no increase in time (left figure of FIG. 8). This modulation is due to the sweeping of the energy flux along the target plate, right figure of FIG. 8. The profiles in the parallel direction on the target plate have a 1 Hz frequency governed by the plasma current. In this experiment, the exhaust energy flux, $Exhaust$ is of the order of $2 MW m^{-2}$ (i.e. well below the design limit). A very different behaviour is noticeable for the surface temperature of the CFC tiles, left figure of FIG. 8. The blue trace is characterised by a steady rise in time. The small temperature increase is due to the small exhaust energy flux to this component, $Exhaust \sim 0.25 MW m^{-2}$. This is indicative of the well-localised power deposition on the high heat flux components.

During the experiments, the plasma modulation was used to control some bright areas visible on the CCD camera viewing the plasma tangentially in visible light. During the shot it could be seen that the brightness of these spots increased with time in an uncontrolled fashion. It was found that the plasma current modulation at 1 Hz led to a modulation of some of the bright spots allowing in some cases to control the rise in brightness. To analyse this behaviour, the CCD film of this pulse was Fourier analysed in time. This gave access to the various time constants that control the in-vessel components, FIG. 9. Two main areas of CCD emission are found ; the area in the vicinity of a lower port with some cooling to protect the port from electron ripple losses and a bottom limiter inertially cooled and withdrawn from the plasma. In the area of the lower port, the bright spots are modulated at 1 Hz, some reach steady emission while others increase and rapidly exceeds the saturation limit of the camera (Left figure on FIG. 9). Points on the limiter do not exhibit the 1 Hz modulation but a slow rise with a time dependence similar to that of the time traces on FIG. 7. The plasma current modulation is thus important to sweep the edge electron beam generated by the LH grill and which interacts with the components in the vicinity of the lower port.

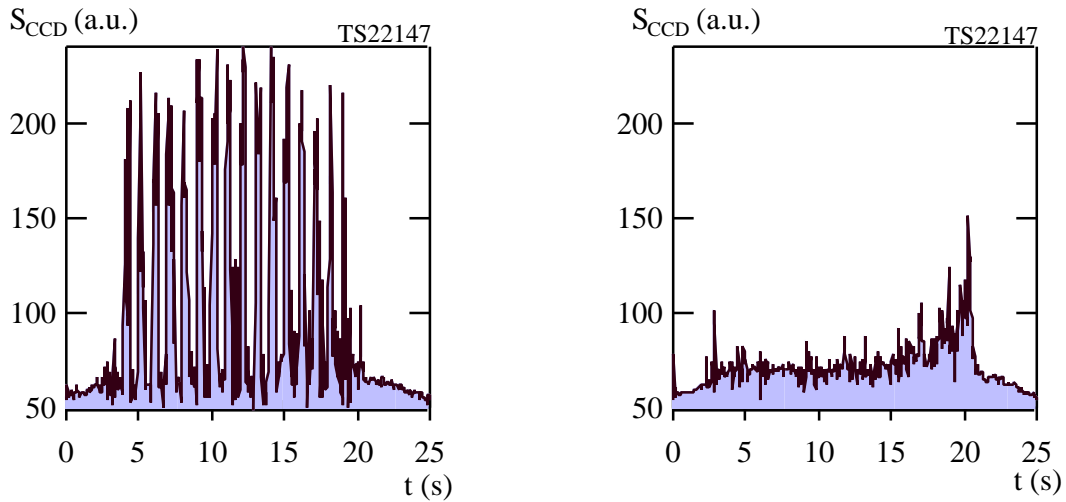


FIG. 9 : Time traces of the two points on the CCD camera viewing the plasma tangentially in visible light. On the left side, point near a port which clear correlation with the 1 Hz modulation of plasma current, on the right, point on an inertial limiter, withdrawn from the plasma.

However, the plasma current modulation does not modify the heating of the inertially cooled bottom limiter. The power law decay of the emission at the end of the shot is characteristic of the temperature relaxation of an inertially cooled component. Strict control of all the in-vessel components, and, in particular cooling to maintain steady state temperature is required to tackle the issue of long pulse operation. This goal is that of the CIEL project presently implemented in Tore Supra [31].

4 Conclusion

Ergodic Divertor operation is characterised by good performance in terms of divertor properties and no deterioration of core performance. From the technological point of view it has operated with actively cooled components, in-vessel coils, with no faults. Power exhaust in particular was eased due to the low parallel energy flux routinely achieved. Furthermore, the ability to operate with a low value of the safety factor, separatrix value ~ 2 has allowed the dedication of 36 % of the volume to open field lines without lowering core confinement and plasma current.

The boundary of stochastic field lines has also permitted coupling of ICRH and LH waves with little difficulty. Additional heating with ICRH was used for high density and radiative divertor operation. Density comparable to the Greenwald density has been achieved. LH power provided the means to address long shot operation. Flat top of the plasma current in the 20 s range has been achieved, and current generation efficiency is also found to be close to that of limiter shots.

In the near future of Ergodic Divertor operation will start on the Textor DED. Symbolically enough, the final shot of the Tore supra ergodic divertor was devoted to simulation of the Textor configuration. A new Ergodic Divertor for Tore Supra is still referred to. However, it would be more valuable for the fusion community to compare ergodic and axisymmetric

divertor in the same device. This would also have the virtue of allowing combined operation, a tempting idea in view of working with a steady state ELMs at the plasma boundary.

References

- [1] Equipe Tore Supra presented by A. Bécoulet, OV2/2, Proc. 17th IAEA Int. Conf., Yokohama 1998, Fusion Energy, IAEA 1998, Vienna 1999, Vol. 1, p. 83-89.
- [2] Ph. Ghendrih, A. Grosman and H. Capes, Theoretical and experimental investigation of ergodic divertor operation on Tore Supra, in *Transport, chaos and Plasma Physics 2*, Editors S. Benkadda, F. Doveil and Y. Elskens, Advanced Series in Nonlinear Dynamics, Vol. 9, World Scientific, Singapore 1996, p.179-193.
- [3] Ph. Ghendrih, A. Grosman & H. Capes, Plasma Phys. Contr. Fusion, **38** (1996) 1653-1724.
- [4] Ph. Ghendrih, H. Capes, F. Nguyen and A. Samain, Contributions to Plasma Physics, **32** (1992) 179-191.
- [5] F. Nguyen, P. Ghendrih, A. Grosman, Nucl. Fusion, **37** (1997) 743-757.
- [6] S. Benkadda et al., Bursty Transport in Tokmaks with Internal Transport Barriers, TH2/2, 18th IAEA Fusion Energy Conference, Sorrento, October 2000.
- [7] W. Fundamenski, P.C. Stangeby, J.D. Elder, J. Nuclear Mater., **266-269** (1999) 1045-1050.
- [8] G. Janeschitz G. Fussmann, P.B. Kotzé, Nucl. Fus., **26** (1986) 1725.
- [9] A. Loarte, R.D. Monk, J.R. Martin-Solis, D.J. Campbell et al., Nucl. Fusion, **38** (1998) 331-371.
- [10] B. LaBombard et al., Cross-field Plasma Transport and Main Chamber Recycling in Diverted Plasmas on Alcator C-mod, to be published in J. Nuclear Mater.
- [11] Ph. Ghendrih, Control of divertor geometry and performance with the Ergodic Divertor of Tore Supra, to be published in J. Nuclear. Mater.
- [12] W.L. Rowan et al., Contribution to 17th EPS conference, Amsterdam 1990, Europhysics Conference Abstracts, (1990) Vol. 14B, p. 26.
- [13] C.S. Pitcher and P.C. Stangeby, Plasma Phys. Contr. Fus., **39** (1997) 779-930.
- [14] Equipe Tore Supra, presented by Ph. Ghendrih, Plasma Phys. Contr. Fusion, **39** (1997) B207-B222
- [15] Y. Nakamura et al., Particle and power balance study in Long Pulses Discharges on LHD, to be published in J. Nuclear Mater.
- [16] M. Goniche, D. Guilhem, P. Bibet, P. Froissard, X. Litaudon, et al., Nuclear Fusion, **38** (1998) 919-937.
- [17] R. Pugno, J.-J. Cordier, Ph. Ghendrih, M. Goniche, A. Grosman, J.P. Gunn, J. Mailloux, S. Person, J. Nucl. Mater., **266-269** (1999) 280-284.
- [18] J. Bucalossi et al., Feedback control on edge plasma parameters with ergodic divertor in Tore Supra, to be published in J. Nuclear. Mater.
- [19] G. Martin et al., Real Time Plasma Feedback Control : An Overview of Tore supra Achievements, EXP1/11, 18th IAEA Fusion Energy Conference, Sorrento, October 2000.
- [20] P. Monier-Garbet et al., High radiation from intrinsic and injected impurities in Tore Supra ergodic divertor plasmas, to be published in J. Nuclear. Mater.
- [21] G.F. Matthews, S. Allen, N. Asakura, J. Goetz, H. Guo et al., J. Nucl. Mater., **241-243** (1997) 450-455.
- [22] Equipe Tore Supra presented by Ph. Ghendrih, Proc. 13th IAEA Int. Conf., Washington 1990, Plasma Physics and Controlled Nuclear Fusion Research, IAEA, Vienna 1991, Vol. 1, p. 549-547.
- [22] M. Zabiégo et al., Characterisation of the separatrix position in the ergodic divertor discharges of the tore supra tokamak, to be published in J. Nuclear. Mater.
- [23] S.M. Kaye, ITER Confinement Database Working Group, Nuclear Fusion, 37 (1997) 1303-1328.
- [24] J. Payan, X. Garbet, J.H. Chatenet et al., Nuclear Fusion, **35** (1995) 1357-1367.
- [25] P. Beyer, X. Garbet and P. Ghendrih, Physics of Plasmas, **5** (1998) 4271-4279.
- [26] P. Devynck et al., Density fluctuations at high density in the Ergodic Divertor configuration of Tore Supra, to be published in J. Nuclear. Mater.
- [27] P. Monier-Garbet, G.T. Hoang, J. Ongena et al., Proc. of the 25th EPS Conference on Controlled Fusion and Plasma Physics, Prague 1998, Europhysics Conference Abstracts, (1998) Vol. 22C.
- [28] F. Nguyen et al., Ergodic divertor experiments in Tore Supra above the Greenwald density limit with ICRF power at low magnetic field, contr. to 27th EPS Conf. on Controlled Fusion and Plasma Physics
- [29] Y. Peysson et al., High Power Lower Hybrid Current Drive Experiment in Tore Supra Tokamak, EX8/2, 18th IAEA Fusion Energy Conference, Sorrento, October 2000.
- [30] C. Grisolia, the Tore Supra team, J. Nuclear Mater., **266-269** (1999) 146-152.
- [31] P. Garin, Tore supra team, CIEL in Tore Supra : how to master power and particles on very long discharges 10th International Toki Conference on Plasma Physics and Controlled Nuclear Fusion, Toki City (Japan), January 2000.